A Novel Approach for On-Line Tuning in the Defuzzification Stage of Fuzzy Logic Controllers

M. Onder Efe[1], Okyay Kaynak[2] and Xinghuo Yu[3]

[1]Carnegie Mellon University, Electrical and Computer Engineering Department
Pittsburgh, PA 15213-3890, U.S.A. efemond@andrew.cmu.edu

[2]Bogazici University, Electrical and Electronic Engineering Department
Bebek, 80815, Istanbul, Turkey, kaynak@boun.edu.tr

[3]Faculty of Informatics and Communication
Central Queensland University, Rockhampton QLD 4702, Australia, x.yu@cqu.edu.au

ABSTRACT

In this paper, a novel method for tuning the parameters of fuzzy controllers is discussed. The aim of the design is to extract a tuning law for the defuzzifier parameters such that the specifications of the control problem are met and the adjustable parameters evolve boundedly. The achievement of these specifications is a challenge in the presence of strong external disturbances, ambiguities in the plant model and nonlinearities, which absolutely require robustness for performance and stability for safety and applicability. The approach introduced in this paper achieves these targets by utilizing the sliding mode control technique based on an augmented switching manifold. The proposed law is applicable to the class of controllers, the output of each member of which is linear in the adjustable parameter set. This stipulates that the fuzzy controllers fall within the application spectrum of the proposed technique. In the application example, fuzzy control of a coupled double pendulum system is considered. The dynamic model of the plant is assumed to be unknown and the difficulties introduced by observation noise and nonzero initial conditions are studied.

1. INTRODUCTION

The problem of tuning the parameters of a controller for meeting a set of predefined performance specifications is a challenge because of the nonlinearities existing in the plant model, disturbances and time varying nature of the processes. Especially if the accuracy in the response is sought, the controller must have a degree of autonomy so that the nonlinear behavior is handled together with disturbance rejection ability. One way of achieving these goals is to use fuzzy control schemes with a suitable adaptation law. From this point of view, integration of Variable Structure Systems (VSS) theory in learning can offer an appropriate solution, which introduces both the robustness and accuracy. In [1-3], it is demonstrated that VSS theory can be used for stabilization and robustification of learning dynamics of computationally intelligent methods. The approach presented in these references is based on the development of a dynamic model for the learning strategy and the design of a sliding motion in the parametric displacement space. The method studied in [1-3] has been utilized in the training of several neural network and fuzzy inference system models used for the purpose of controlling robotic manipulators.

Another pioneering work through the direction of using VSS theory in learning process is presented in [4]. In this reference, a particular treatment is developed for Gaussian networks. In [5], similar to the viewpoint of Sanner *et al* [4], a dual mode adaptive controller is developed by using Gaussian networks and a stability analysis is presented in detail. The results discussed in [5] stipulated that good transient and steady state responses could be obtained.

Some studies on the use of SMC strategy are devoted to the dynamic adaptation of the parameters of a flexible model such that the error on the output of the model tends to zero in finite time [6]. Yu *et al* [7] extend the results of [6] by introducing adaptive uncertainty bound dynamics and focus on the same example as the application. The major drawback in both of the approaches is the fact that the dynamic adaptation mechanism needs the error on the output of the flexible structure. If the structure is to be used as a controller, this fact constitutes a difficulty because the use of the approaches proposed in [6-7] for control applications require the error on the control signal to be applied, which is unavailable. The second drawback of the dynamic uncertainty bound adaptation strategy in [7] is the existence of noise on the measured variables. The approach in [7] requires the integration of the absolute value of the error signal observed on the outputs. When the error signal is close to zero, it clearly leads to the integration of the absolute value of the noise signal, which gradually increases the bound value and leads to instability in the long run.

In [8-9], it is presented that the original form of the method discussed by Ramirez *et al* [6] can be used for control applications, in which the target output of the intelligent system, i.e. the controller, is unknown. The major difference of what is presented in this paper from what has been discussed in the literature is the construction of a dynamic adaptation law based on a switching manifold, which is augmented with the sensitivity derivatives of an appropriately defined cost function. The paper analyzes the relation between the sliding surface for the plant to be controlled and the zero learning error level for the output of a flexible controller.

The organization of the paper is as follows: The second section gives the definitions and the formulation of the problem and derives the first critical value of the uncertainty bound parameter denoted by *K*. The following section introduces the equivalence constraints on the sliding control performance for the plant and sliding mode learning performance for the controller. The section gives the second critical value of *K* and combines the two constraints. The fourth section describes the dynamic model of the plant used in the simulations and presents the simulation studies. Conclusions constitute the last part of the paper.

2. PARAMETER TUNING BASED ON A TWO-TERM LYAPUNOV FUNCTION

In this section, an analysis of the sliding mode creation problem, which is based on a two-term Lyapunov function, is given. The proposed form of the update dynamics constructs the time derivative of the parameter vector, the use of which results in the observation of a sliding mode taking place after a reaching mode on the phase plane.

Consider a 2-input single output Fuzzy Logic Controller (FLC) with *R* rules described as

$$\tau = \underline{\phi}^T \underline{w}_n \tag{1}$$

where, $\underline{\phi}$ is the vector of defuzzifier weight, which is of dimensions Rx1, and $\underline{w}_n$ is the normalized vector of firing strengths. The i^th entry of the latter is given in (2), and the input vector is given in (3).

$$w_{n\,i} = \frac{\prod_{j=1}^{2} \mu_{ij}\left(u_j\right)}{\sum_{k=1}^{R} \prod_{j=1}^{2} \mu_{kj}\left(u_j\right)} \tag{2}$$

$$\underline{u} = \begin{bmatrix} e & \dot{e} \end{bmatrix}^T \tag{3}$$

In above, the symbol e denotes the tracking error, which is the discrepancy between the response of the system under control (x) and the reference signal (x_d), i.e. $e = x - x_d$. The structure of the control system is an ordinary feedback loop as illustrated in Fig. 1. The definitions of the sliding line s_p and that of zero learning-error level s_c, which are seen in this figure, are described as

$$s_p\left(e, \dot{e}\right) = \dot{e} + \lambda e \tag{4}$$

where, λ is the slope of the sliding surface and

$$s_c\left(\tau, \tau_d\right) = \tau - \tau_d \tag{5}$$

where, τ_d is the desired output of the controller and is unknown. Based on these definitions, one can define the following quantity as the cost measure,

$$J = \frac{1}{2} s_c^2 \tag{6}$$

which instantly qualifies the similarity between the produced control signal and its desired value. Using this measure, an augmented switching manifold can be designed as in (7), and a Lyapunov function can be constructed as in (8).

$$\underline{s}_A = \begin{bmatrix} s_c \\ \dfrac{\partial J}{\partial \underline{\phi}} \end{bmatrix} \tag{7}$$

$$V_c = \frac{1}{2} \underline{s}_A^T P \underline{s}_A \tag{8}$$

where, *P* is defined as follows.

$$P = \begin{bmatrix} \zeta & \underline{0}_{1x(m+1)} \\ \underline{0}_{(m+1)x1} & \rho I_{(m+1)x(m+1)} \end{bmatrix} \tag{9}$$

where, ζ and ρ are positive constants. Based on the selection in (9), the open form of the Lyapunov function in (10) can be written as follows.

$$V_c = \zeta J + \rho \frac{1}{2} \left\| \frac{\partial J}{\partial \underline{\phi}} \right\|^2 \tag{10}$$

in which, the selection of the weight parameters ζ and ρ must be done by comparing the magnitudes of the time-varying two terms of (10). For a vector denoted by $\underline{\nu}$, the definition of the norm used in (10) can be given as $\left\|\underline{v}\right\| = (\underline{v}^T \underline{v})^{1/2}$.

In order not to violate the constraints of the physical reality, the following boundedness conditions are imposed.

$$\left\|\underline{\phi}\right\| \le B_{\phi} \tag{11}$$

$$\left\|\underline{w_n}\right\| \le B_{w_n} \tag{12}$$

$$\left\|\underline{\dot{w}_n}\right\| \le B_{\dot{w}_n} \tag{13}$$

$$\|\;\| \quad \tau$$

$$\left\|\tau_d\right\| \le B_{\tau_d} \tag{15}$$

$$\left\|\dot{\tau}_d\right\| \le B_{\dot{\tau}_d} \tag{16}$$

The numerical values of these bounds are not certain in most of the applications but the realistic design approaches must take them into consideration as they determine the domain of applicability of a strategy.

***Theorem* 1.** For a controller structure, in which the output is a linear function of the adjustable parameters, the adaptation of the controller parameters as described in (17) ensures the negative definiteness of the time derivative of the Lyapunov function candidate in (10).

$$\dot{\underline{\phi}} = -K\left(\zeta I + \rho \frac{\partial^2 J}{\partial \underline{\phi}\, \partial \underline{\phi}^T}\right)^{-1} \mathrm{sgn}\left(\frac{\partial J}{\partial \underline{\phi}}\right) \tag{17}$$

where, K is a sufficiently large constant satisfying (18).

$$K > K_{cr1} = \left(\zeta B_{\phi} + \rho B_{w_n}\right) B_{\dot{w}_n} \tag{18}$$

where, K_{cr1} is the first critical lower bound of the uncertainty bound parameter K. A brief proof of the theorem is given in (19), for detailed explanation, the reader is referred to [8].

$$\begin{aligned}
\dot{V}_c &\le -K s_c \underline{w_n}^T \mathrm{sgn}\left(s_c \underline{w_n}\right) + \left(\zeta B_{\phi} + \rho B_{w_n}\right) B_{\dot{w}_n} \left|s_c\right| \\
&= -K\left|s_c\right| \underline{w_n}^T \mathrm{sgn}\left(\underline{w_n}\right) + \left(\zeta B_{\phi} + \rho B_{w_n}\right) B_{\dot{w}_n} \left|s_c\right| \\
&= -\left|s_c\right|\left(K \underline{w_n}^T \mathrm{sgn}\left(\underline{w_n}\right) - \left(\zeta B_{\phi} + \rho B_{w_n}\right) B_{\dot{w}_n}\right) \\
&\le -\left|s_c\right|\left(K - \left(\zeta B_{\phi} + \rho B_{w_n}\right) B_{\dot{w}_n}\right)
\end{aligned} \tag{19}$$

3. ANALYSIS OF THE EQUIVALENCE BETWEEN SLIDING MODE CONTROL AND SLIDING MODE LEARNING

Consider the sliding line s_p and the zero-learning-error level s_c described by (4) and (5) respectively. The relation between these two quantities is assumed as in (20).

$$s_c = \Psi\left(s_p\right) \tag{20}$$

Qualitatively, if the value of s_p tends to zero, this means that s_c goes to zero. Theoretically, the system achieves perfect tracking because the controller produces the desired control inputs or vice versa. Conversely, as the value of s_p increases in magnitude, indicating that the error vector is getting away from the origin, the same sort of a divergent behavior in s_c is observed or vice versa. The details in postulating the form of the relation Ψ are presented in [9].

***Theorem* 2.** All monotonically increasing continuous functions passing through the origin can serve as the Ψ relation for the establishment of an equivalence between the sliding mode control of the plant and the sliding mode learning inside the controller.

$$\begin{aligned}
\dot{V}_p &= \dot{s}_p s_p \\
&= \left(\overset{\bullet}{\Psi^{-1}\left(s_c\right)}\right)\Psi^{-1}\left(s_c\right) \\
&= \frac{\partial \Psi^{-1}\left(s_c\right)}{\partial s_c}\dot{s}_c \Psi^{-1}\left(s_c\right) \\
&= \frac{\partial \Psi^{-1}\left(s_c\right)}{\partial s_c}\left(\dot{\underline{\phi}}^T \underline{w_n} + \underline{\phi}^T \underline{\dot{w}_n} - \dot{\tau}_d\right)\Psi^{-1}\left(s_c\right) \\
&\le \frac{\partial \Psi^{-1}\left(s_c\right)}{\partial s_c}\left|\Psi^{-1}\left(s_c\right)\right|\left(B_{\phi} B_{\dot{w}_n} + B_{\dot{\tau}_d}\right) + \\
&\quad -\frac{\partial \Psi^{-1}\left(s_c\right)}{\partial s_c}\left|\Psi^{-1}\left(s_c\right)\right|\frac{K}{\zeta}\left(1 - \frac{\rho \underline{w_n}^T \underline{w_n}}{\zeta + \rho \underline{w_n}^T \underline{w_n}}\right) \\
&< \frac{\partial \Psi^{-1}\left(s_c\right)}{\partial s_c}\left|\Psi^{-1}\left(s_c\right)\right|\left(B_{\phi} B_{\dot{w}_n} + B_{\dot{\tau}_d}\right) + \\
&\quad -\frac{\partial \Psi^{-1}\left(s_c\right)}{\partial s_c}\left|\Psi^{-1}\left(s_c\right)\right|\frac{K}{\zeta + \rho} \\
&< 0 \Leftrightarrow K > K_{cr2} = \left(B_{\phi} B_{\dot{w}_n} + B_{\dot{\tau}_d}\right)\left(\zeta + \rho\right)
\end{aligned} \tag{21}$$

It is now clear that there are two critical lower bound values for the uncertainty bound parameter K, and the formulation of these values are seen in (18) for K_{cr1}, and in the last line of (21) for K_{cr2}. In (22), the two constraints on the design parameter K are combined.

$$K > \max\left(K_{cr1}, K_{cr2}\right) \tag{22}$$

Apparently the selection of the bound parameter as given in (22) enforces the value of s_c to zero level, or equivalently, s_p to zero.

4. SIMULATION STUDIES

In this study, a coupled double pendulum system is used to elaborate the performance of the method discussed. The physical structure of the plant is illustrated in Fig. 2. Since the dynamics of such a mechatronic system is modeled by nonlinear and coupled differential equations, precise tracking becomes a difficult objective due to the strong interdependency between the variables involved. Furthermore, the ambiguities introduced by the noise on the measured quantities make the design of a robust controller so complicated that the achievement of which is a challenge in conventional design framework. Therefore, for such a system, the control methodology adopted must be capable of handling the difficulties stated.

The differential equations characterizing the behavior of the system are given in (23)-(26), in which the angular positions and the angular velocities define the state vector. The control inputs, which are denoted by τ_1 and τ_2, are provided to the relevant pendulum by the base servomotors. The parameters of the plant are given in Table 1.

$$\dot{x}_1 = x_3 \tag{23}$$

$$\dot{x}_2 = x_4 \tag{24}$$

$$\dot{x}_3 = \left(\frac{M_1 g r}{J_1} - \frac{k_s r^2}{4 J_1} \right) \sin(x_1) + \frac{k_s r}{2 J_1}(l - b) + \frac{\tau_1}{J_1} + \frac{k_s r^2}{4 J_1} \sin(x_4) \tag{25}$$

$$\dot{x}_4 = \left(\frac{M_2 g r}{J_2} - \frac{k_s r^2}{4 J_2} \right) \sin(x_2) + - \frac{k_s r}{2 J_2}(l - b) + \frac{\tau_2}{J_2} + \frac{k_s r^2}{4 J_2} \sin(x_3) \tag{26}$$

where, g=9.81 m/s^2 is the gravitational acceleration constant. As given in Table 1, since $b<l$, the two pendulums repel each other in the upright position. The model introduced in this section has been studied by Spooner and Passino [10], who discuss the decentralized adaptive control using radial basis neural networks.

In the simulation studies presented, the plant introduced is controlled by the proposed control scheme. The aim is to produce some control signals such that the application of which results in the observation of a sliding motion in the phase plane. As the controller, the architecture described by (1) is utilized with w_{ni} being as described in (2). The structure of the control system is illustrated in Fig. 2, in which the plant is in an ordinary feedback loop. Based on the tracking error vector, first the value of s_p is evaluated and this quantity is passed through the Ψ function to get the value of s_c, which is used in the dynamic adjustment mechanism. In evaluating the value of the quantity s_p, the slope parameter of the switching line (λ) has been set to unity for both FLC controllers, which have bell-shaped membership functions and 9 rules (R=9) in the rule base.

In practical implementations of control structures for trajectory control of mechatronic devices, a number of difficulties are encountered, which make it difficult to achieve an accurate trajectory tracking. The simulation studies carried out address these difficulties. The first difficulty to be alleviated is the existence of the observation noise. To study the effects of this situation, which is very likely to be encountered in practice, the information used by the controller is corrupted by a Gaussian distributed random noise having zero mean and variance equal to 0.33e-6. The peak magnitude of the noise signal is within ±1e-3 with probability very close to unity. The second difficulty is the nonzero positional initial conditions. In order to demonstrate the reaching mode performance of the algorithm, the initial positional errors have been set to $-\pi/12$ radians and $\pi/12$ radians for the first and the second pendulums respectively. The reference trajectory used in the simulations is depicted in Fig. 3.

It should be pointed out that once the error or the rate of error comes very close to zero, the adjustment mechanism is driven solely by the noise signal corrupting the observed state variables. Since the bound of perturbing signal is known, the update law described in (17) can be modified such that the adverse effects of noise driven parameter tuning activity are reduced. This can be achieved by utilizing a sufficiently hard threshold function given by (27). The value of threshold is denoted by n_b and has been set to 2e-3 in the simulations. The modified form of the update equation in (17) is given in (28).

$$T(s_p) = \left(1 + \exp\left(-10^5\left(|s_p| - n_b\right)\right)\right)^{-1} \tag{27}$$

$$\dot{\underline{\phi}} = -K\left(\zeta I + \rho \frac{\partial^2 J}{\partial \underline{\phi}\, \partial \underline{\phi}^T}\right)^{-1} \mathrm{sgn}\left(\frac{\partial J}{\partial \underline{\phi}}\right) T(s_p) \tag{28}$$

As the Ψ relation, the following selection is made parallel to the remarks presented in the fourth section.

$$\Psi(s_p) = s_p \tag{29}$$

Furthermore, in order to reduce the chattering effect in the sliding mode, the function in (30) has been used instead of the sgn function in the dynamic strategy described in (28), and initially, the adjustable parameters are all set to zero.

$$\mathrm{sgn}(\Psi(s_p)) \approx \frac{\Psi(s_p)}{|\Psi(s_p)| + 0.05} \tag{30}$$

Under these conditions, the state tracking error graph in Fig. 4 is obtained. The trend in position and velocity errors clearly stipulate that the algorithm is capable of achieving precise tracking objective with a sufficiently fast response characterized by λ. The applied control signals are depicted in Fig. 5, in which the smoothness of the signals is another important property. The motion in the phase plane is illustrated in Fig. 6, in which after a fast reaching mode, a sliding mode is enforced and is maintained by producing a suitable control signal. Lastly, the behaviors of the parameters of the two controllers are illustrated in Figs. 7 and 8, from which the bounded evolution is clear.

During the simulations, the bounds for the uncertainties denoted by K for both pendulums have been set to 800. The weight parameters ζ and ρ have been selected as unity for both FLCs. The simulation stepsize has been selected as 2.5 msec and the time required to perform the simulation has been measured as 91 seconds on a Pentium III-600 PC running Matlab 5.3 software. This indicates that the complexity of the algorithm in real time control applications is dependent on the speed of the chosen DSP interface, the widespread examples of which operates machine coded algorithms and performs thousands of floating point operations in a few milliseconds as they do not have to run heavy operating systems.

6. CONCLUSIONS

In this paper, a novel method for establishing a sliding motion in the dynamics of a nonlinear plant is discussed. The method is based on the adoption of a nonlinear dynamic adjustment strategy in a controller structure, whose output is a linear in the adjustable parameters. The task is to drive the tracking error vector to the sliding manifold and keep it on the manifold forever. What makes the proposed algorithm so attractive in this sense is the fact that the sliding mode control of the plant is achieved while an equivalent regime is imposed on the controller parameters. Contrary to what is known in the field of variable structure controller design, the governing equations of the plant under control are assumed to be unknown and the lack of this knowledge is left as a difficulty to be alleviated by a learning controller.

As discussed throughout the paper, the problems that arise due to the uncertainties are alleviated by incorporating the robustness provided by the VSS technique into the proposed approach. A further attractiveness of the algorithm is the fact that the controller for each pendulum possesses only R adjustable parameters for the application example considered. The computational requirement for FLC realization is not therefore excessive.

Finally, the simulation results presented demonstrate that the algorithm discussed is able to compensate deficiencies caused by the imperfect observations of the state variables, nonzero initial errors and complex plant dynamics. From these points of view, the method proposed is highly promising in control engineering practice.

ACKNOWLEDGMENTS

This work is supported by Bogazici University Research Fund (Project no: 00A203D)

REFERENCES

[1] Efe M. O., O. Kaynak and B. M. Wilamowski, “Stable Training of Computationally Intelligent Systems By Using Variable Structure Systems Technique,” *IEEE Trans. on Industrial Electronics*, v.47, no.2, pp.487-496, 2000.

[2] Efe M. O. and O. Kaynak, “Stabilizing and Robustifying the Learning Mechanisms of Artificial Neural Networks in Control Engineering Applications,” *Int. Journal of Intelligent Systems*, v.15, no.5, pp.365-388, 2000.

[3] Efe, M. O. and Kaynak, O., “On Stabilization of Gradient Based Training Strategies for Computationally Intelligent Systems”, to appear in *IEEE Transactions on Fuzzy Systems*, v.8, no.5, pp.564-575, 2000.

[4] Sanner, R.N. and J.J.E. Slotine, “Gaussian Networks for Direct Adaptive Control,” *IEEE Transactions on Neural Networks*, v.3, no.6, pp.837-863, 1992.

[5] Hsu, L. and J. A. Real, “Dual Mode Adaptive Control, ” Proceedings of the IFAC'99 World Congress, v.K, pp.333-337, Beijing, July 1999.

[6] Sira-Ramirez, H. and E. Colina-Morles, “A Sliding Mode Strategy for Adaptive Learning in Adalines,” *IEEE Trans. on Circuits and Systems – I: Fundamental Theory and Applications*, v.42, no.12, pp.1001-1012, 1995.

[7] Yu, X., M. Zhihong and S. M. M. Rahman, “Adaptive Sliding Mode Approach for Learning in a Feedforward Neural Network,” *Neural Computing and Applications*, v.7, pp.289-294, 1998.

[8] Efe, M. O., Variable Structure Systems Theory Based Training Strategies for Computationally Intelligent Systems, Ph.D. Thesis, Bogazici University, 2000.

[9] Efe, M. O., O. Kaynak and X. Yu, “Sliding Mode Control of a Three Degrees of Freedom Anthropoid Robot by Driving the Controller Parameters to an Equivalent Regime,” *Trans. of the ASME: Journal of Dynamic Systems, Measurement and Control*, v.122, no.4, pp.632-640December 2000.

[10] Spooner, J. T. and K. M. Passino, “Decentralized Adaptive Control of Nonlinear Systems Using Radial Basis Neural Networks,” *IEEE Trans. on Automatic Control*, v.44, no.11, pp. 2050-2057, 1999.

Table 1. Plant Parameters

Mass of pend. 1	M_1	2 kg
Mass of pend. 2	M_2	2.5 kg
Moment of inertia for pend. 1	J_1	0.5 kg
Moment of inertia for pend. 2	J_2	0.625 kg
Spring constant	k_s	100 N/m
Natural length of the spring	l	0.5 m
Distance between pend. hinges	b	0.4 m
Pendulum height	r	0.5 m

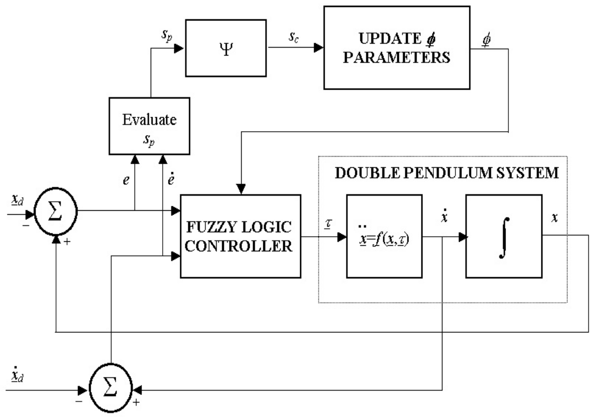

Figure 1. Structure of the Control System

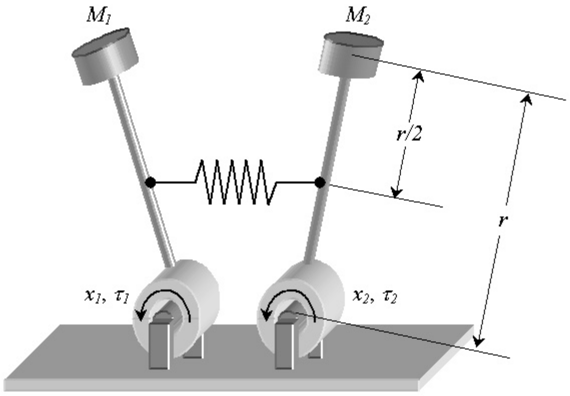

Figure 2. Physical Structure of the Double Pendulum System

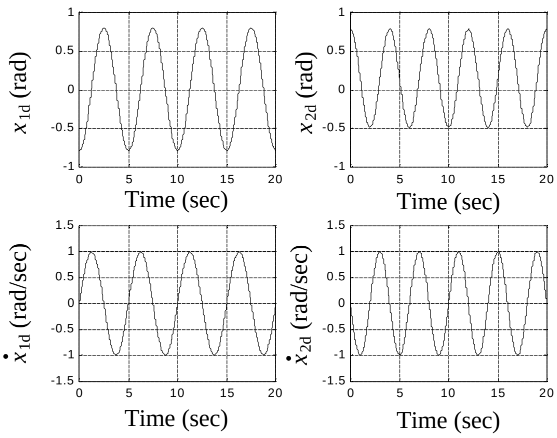

Figure 3. Reference State Trajectories

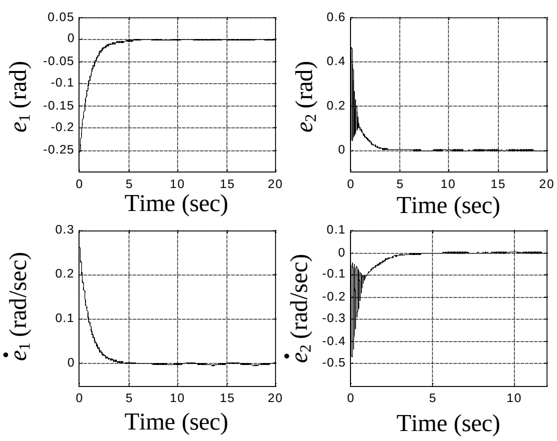

Figure 4. State Tracking Errors

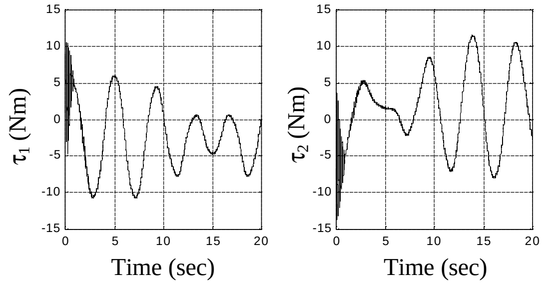

Figure 5. Applied Control Signals

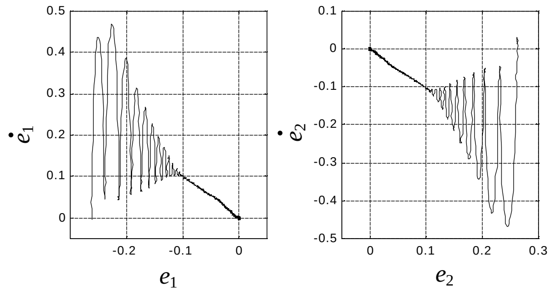

Figure 6. Trajectories in the Phase Plane

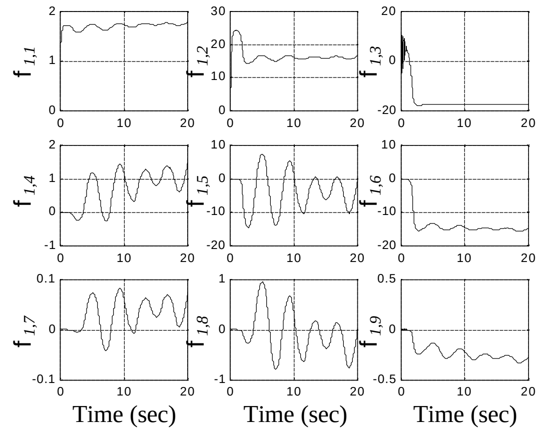

Figure 7. Evolution of the Parameters of the First Pendulum Controller

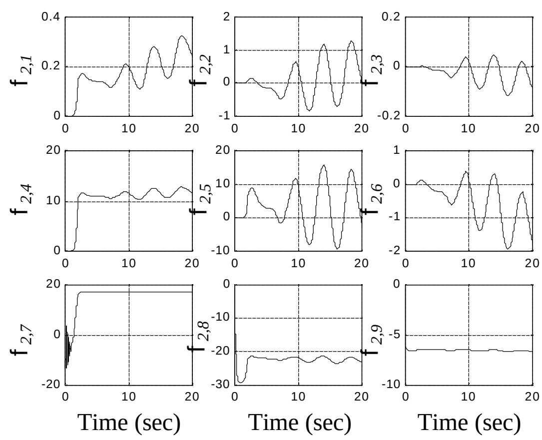

Figure 8. Evolution of the Parameters of the Second Pendulum Controller